Design and Numerical Investigations of a Deep Excavation for a Tunnel Entrance Pit

Planification et calculs numériques pour une excavation profonde pour la construction de l'entrée d'un tunnel

M. Raithel

Kempfert + Partner Geotechnical Engineering Consultants, Würzburg/Kassel, Germany

Berhane Gebreselassie

Institute of Geotechnics and Geohydraulics, University of Kassel, Germany

S. Müller, F. Pahl

Hochtief Construction AG, Hamburg, Germany

ABSTRACT

For the crossing of the Trave river in Lübeck, Germany, a new shield tunnel is constructed to replace the existing Bridge. At its entrance the tunnel changes into an open 130 m long pit. In order to carry out the excavation of the open pit, it was necessary to remove the existing access road of the bridge and redirect the existing federal highway to a temporarily constructed road on a 12.5 m high cofferdam. This results in a total height difference of about 25 m from the top of the cofferdam to the bottom of the open excavation. In order to analyse the unpredicted deformations during the execution of the excavation, a numerical analysis of the excavation was performed. The paper presents the construction and design of the retaining structures together with the 12.5 m high cofferdam and shows a detailed description of the boundary conditions and the execution of the numerical computations. Typical result of the field measurement are graphically plotted and described in comparison with the results of the numerical computations. Finally, the measures required for the completion of the excavation without any danger of excessive deformations are discussed and presented.

RÉSUMÉ

Pour la nouvelle traversée de la Trave, un tunnel avec avancement au bouclier est construit. A l'entrée du tunnel, celui-ci se transforme en trémie ouverte, laquelle est caractérisée par un décrochement de niveau d'une hauteur globale de plus de 25 m. Pour l'analyse de déformations non prévisibles auparavant lors de l'élaboration des fouilles nécessaires, des examens numériques ont été effectués. Dans l'article, la réalisation des calculs numériques est expliquée après la présentation de la construction et le dimensionnement de l'enceinte des fouilles, et les résultats de mesure déterminants sont comparés aux résultats des calculs numériques. Enfin, les déformations survenues sont évaluées.

1 INTRODUCTION

For the crossing of the Trave river in Lübeck, Germany, a new shield tunnel is constructed to replace the existing Bridge. At its entrance the tunnel changes into an open 130 m long pit. An overview of the construction site is shown in Fig. 1.
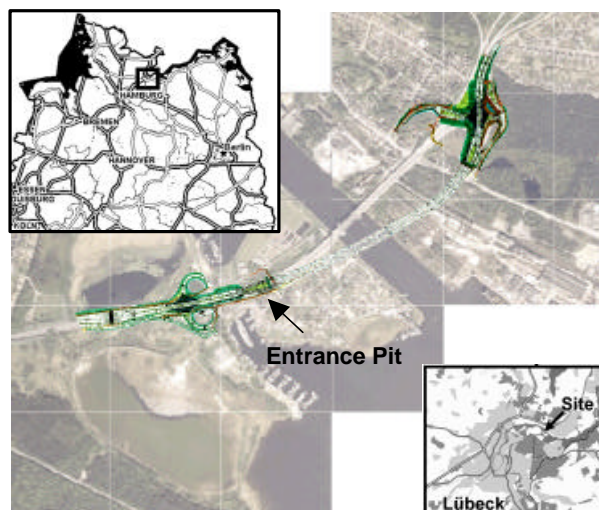

Figure 1: An overview of the construction site

In order to carry out the excavation of the open pit, it was necessary to remove the existing access road of the bridge and redirect the existing federal highway to a temporarily constructed road on a 12.5 m high cofferdam. Thereby results a total height difference of about 25 m from the top of the cofferdam to the bottom of the open excavation. Fig. 2 shows a typical section through the excavation pit.

The excavation is partly supported by a fourfold anchored, 27 m deep and 80 cm thick diaphragm wall which has a free height of about 12.5 m.

At a distance of 8 m behind the wall, a 15 m wide and 12.5 m high (reference: diaphragm wall head) cofferdam made of tied back soldier piles was constructed before the beginning of the excavation on which the federal highway temporarily runs.

For the excavation of the pit, it was first intended to execute the excavation under water, to place underwater concrete at the bottom of the excavation and to pump out the water later. However, due to unexpected soil conditions found in-situ, the original plan was changed in favour of a stepwise lowering of the groundwater in the pit and subsequent excavation. The effect of the groundwater lowering together with the effect of the nearby cofferdam had subjected the retaining structure to a substantial load.

2 SOIL CONDITIONS

The underground is characterised by a succession of sand, basin silt and boulder clay. In general, the layers have a sufficient load bearing capacity. The basin silt, however, exhibits unfavourable bearing and deformation behaviour compared to the overlying and underlying layers. The essential soil parameters of the governing soil layers are given in Table 1. The constrained modulus in Table 1 is at a reference pressure of $p^{ref} = 100$ kN/m².

Because of the close distance of the excavation pit to the Trave river, the groundwater condition is strongly influenced by the water level of the river. The groundwater is characterised by

two different aquifers which are independent from each other. The lower aquifer is found to be confined.

Table 1: Soil parameters at the excavation pit

Soil layer	Unit weight γ/γ' [kN/m³]	Friction angle φ' [°]	Cohesion c' [kN/m²]	Constrained modulus E_s [MN/m²]
Sand fill	19/11	37.5°	0	50
Upper sand	19/11	37.5°	0	50
Basin silt	19/20	25.0°	20	20 - 25
Boulder clay	22/22	30.0°	20	30
Lower sand	19/21	37.5°	0	50

3 EXCAVATION PIT

3.1 *Design and construction*

The part of the retaining structure presented here consisted in the original design a 0,8 m thick diaphragm wall supported at two positions with ground anchors. The anchors were selected according to DIN 4125 and prestressed to about 85% of the service load. Also the wall was assumed to be supported by bottom concrete slab placed under water and has a thickness of 0.8m.

The governing load on the wall comes from the nearby 12.5 m high cofferdam beside to the 12.5 m deep excavation. The design of the wall was performed according to the analytical methods with the program Q-WALLS. As a structural system, the wall was assumed as a beam on an elastic foundation.

Due to the a change of the construction procedure from excavation under water to the gradual lowering of the groundwater followed by dry excavation, the load and support condition of the wall was considerably changed. This results in a gradual increase of the water pressure, and absent of the unyielding bottom concrete slab.

Consequently a redesign of the construction was necessary. It was impossible to increase the bending capacity of the already installed diaphragm wall. Hence, the excessive load on the wall due to the change of the excavation steps should be exclusively carried by additional support systems. A prop support against the opposite wall was not economical for a reason of operation and construction problems. Therefore, the additional required wall support was realized by two additional ground anchors. The anchors were installed and prestressed after each respective excavation stage. A cross section of the new system is shown in Fig. 2.

The determination of the new section forces and deflection of the wall was carried out using the same static system and the same computational program. The design of the now 4times tied back diaphragm wall considered the prestress and the yielding effect of the ground anchors based on the effective elastic anchor length. Moreover, the deformation of the wall in the current construction stage was considered in the design of the wall in the next stage.
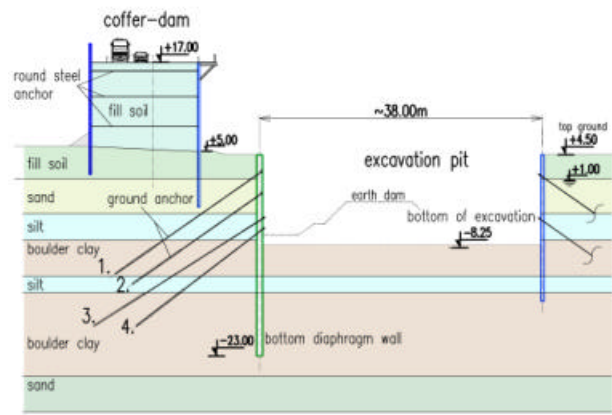

Figure 2: Cross section of the excavation after the redesign

Because of the additional support, no higher deflection of the wall was observed as expected after the change of the construction process. The displacement of the wall, however, could not be predicted using the analytical method, because the program is based on the elastic deflection of the wall and the anchor only.

3.2 *Construction stages and monitoring*

At the time of re-planning of the excavation steps and redesign of the support system, the walls and the upper first and second anchors were already in place. For the evaluation of the stability and safety of the cofferdam standing under continuous traffic load, a monitoring program was installed (see Fig.3). This includes:
- measurement of the position of the head of the tie rods of the cofferdam anchorage in order to determine the change in position and inclination of the cofferdam,
- measurement of the elongation of the tie rod in order to control the stresses in the tie rod and the cofferdam,
- measurement of the deformation of the adjacent diaphragm wall using vertical inclinometer.
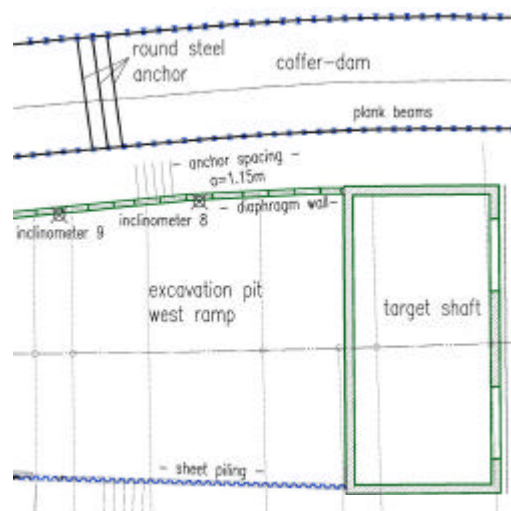

Figure 3: Top view of the excavation site around the diaphragm wall and location of the inclinometer

An observation and limit values of the yield of the anchor and the deformation of the diaphragm wall were specified in order to evaluate continuously the safety of the cofferdam and the excavation. The observation and limit values of the deformation of the wall were determined on basis of the analytical method of computation of the section forces and the

deformation of the diaphragm wall. In the course of the third excavation stage and the installation of the third ground anchor, it was observed that the deformation of the wall exceeded the limit value. The measurements clearly showed that the entire diaphragm wall leaned towards the excavation.

In order to analysis the measured deformation of the wall and hence to judge the safety of the cofferdam and the excavation, a numerical analysis was carried out using the finite element method as described in section 4. Since a good agreement was achieved between the measured and computed deformation of the wall, new observation and limit values were derived on the basis of the FE-results for the inclinometer and anchor force measurements of the diaphragm wall for consequent excavation stages.

At the end of the excavation (last step), the measured wall deformations reached at most about 70% of the computed values. Similarly, the measured anchor forces were about 92% of the computed values. Furthermore, the execution of rest of the excavation was safeguarded by the following additional safety measures:

- measurement of the position of the head of the ground anchor of the diaphragm wall to control the plausibility of the inclinometer measurement,
- installation of load transducers in the 3rd and 4th ground anchor position to control the anchor forces,
- construction and demolishing of earth walls in sections at the respective excavation level to reduce the possible deformation increment between the time of the execution of the new excavation level and the installation and pre-stressing of the respective anchor,
- placement of 40 cm thick reinforced concrete slab as a bottom support to the wall to reduce the possible deformation of the wall after the end of the excavation.

Through the above construction and monitoring measures, it was able to safeguard the safety of the excavation and the cofferdam during the entire construction and utilisation phases.

4 NUMERICAL ANALYSIS

4.1 The FE-Model

The numerical analysis of the excavation were performed with the FE-program "PLAXIS" (finite element code for soil and rocks). A 15 node triangular element was used to generate the model mesh. The FE-model geometry is 235 m long and 112 m high and considers the maximum depth of the excavation. The cross section was selected at the location of the inclinometer 9. The model comprises of 3395 elements, 27769 nodes and 40728 stress points.

An advanced constitutive soil model known as the hardening soil model (HSM) was used to simulate the soil behavior under excavation. The HSM is developed based on the so called the Duncan Chang hyperbolic model. It, however, supersedes the hyperbolic model, because it uses the plasticity theory, it includes the dilatancy soil behavior and it introduces the yield cap. The HSM also considers the stress dependent stiffness of the soil according to the power. For the primary deviatoric loading, the power low is given by

$$E_{50} = E_{50}^{ref} \left(\frac{c' \cdot cos\bm{j} - \bm{s}_3' \cdot sin\bm{j}}{c' \cdot cos\bm{j} + p^{ref} \cdot sin\bm{j}} \right)^m \qquad (1)$$

where E_{50}^{ref} is the secant modulus at 50% of the failure stress and at effective reference pressure of p^{ref} and m is the exponent and it is dependent on the type of the soil.

Similarly, for the un/relaoding

$$E_{ur} = E_{ur}^{ref} \left(\frac{c' \cdot cos\bm{j} - \bm{s}_3' \cdot sin\bm{j}}{c' \cdot cos\bm{j} + p^{ref} \cdot sin\bm{j}} \right)^m \qquad (2)$$

where E_{ur}^{ref} is the un/reloading stiffness at a reference pressure of p^{ref}. For detail information on the constitutive model and the program refer to Gebreselassie (2003) und Vermeer & Brinkgreve (1998).

The soil parameters required for the HSM are taken from Table 1 and the exponent $m = 0.5$ was selected for the sand and basin silt layer and $m = 0.7$ for the boulder clay layer.

The walls, the bottom concrete slab and the soldier piles (cofferdam) are simulated as beam element with linear elastic material behavior. An equivalent thickness of the soldier and sheet pile is derived based on the stiffness and the geometry of the respective walls. Interface elements are introduced between the walls and the soil with a fictitious thickness. The shear strength at the contact surface is assumed to reduce by 50% of the surrounding soil, where as the stiffness of the contact surface remained unchanged.

The groundwater table in the upper aquifer is taken to be at a depth of 3.5 m below the surface and the lower confined aquifer at 4.5 m below the surface.

4.2 Calculation phase

The FE-computations were carried out for the different construction stages. First the pre-loading history of the underground by the existing road embankment was simulated and the primary state of the stresses was defined in this condition. Then followed the installation of the cofferdam, placement of the tie rod, placement of the sand fill into the cofferdam and removal of the existing embankment. Finally, the calculation proceeded by simulating the different excavation phases followed by the installation and pre-stressing of the respective ground anchors. The different construction stages considered in the calculation are shown in Fig. 4.
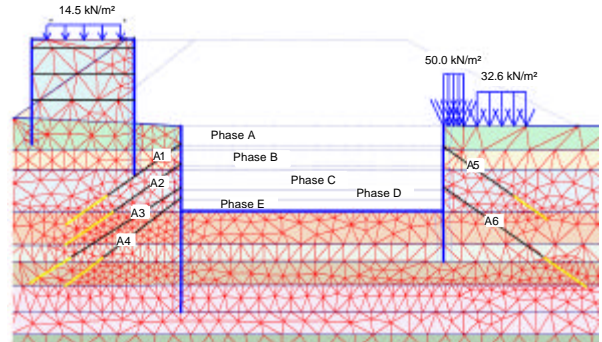

Figure 4: FE-model (detail) and construction stages

The undrained behavior of the underground and the consolidation process was neglected in this numerical computations. Thus, all computed deformations should be regarded as final deformations.

From the numerical analysis, it was observed that the pre-loading of the underground by the existing road embankment had a significant influence on the computations results. This is primarily because the used constitutive soil model is capable of simulating the substantial pre-loading history and the corresponding increase in the stiffness of the underground.

Subsequent to the deformation analysis of the final excavation stage (Phase E), a safety analysis was performed using the Phi-c-reduction option in the "PLAXIS" program to examine the global stability of the excavation.

5 COMPUTATION RESULTS

From Fig. 5 can be shown that the maximum total deformation u at the end of the final stage of the excavation occur at the excavation level on the side of the diapragm wall.
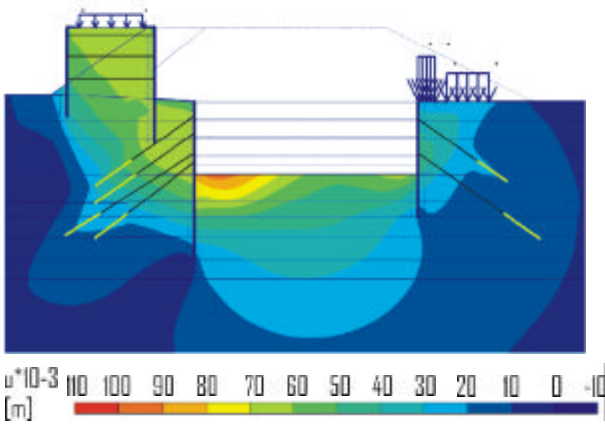
Figure 5: Shadings of the computed total deformation at the end of the final excavation.

The comparison of the measured and the computed deformation of the diaphragm wall at a section through the inclinometer 9 is given in Fig. 6.

At the section through the inclinometer 9, a max. horizontal deformation of the diaphragm wall of 25 mm was computed in comparison to 15 mm measured deformation at the end of the excavation phase C (Fig. 6).
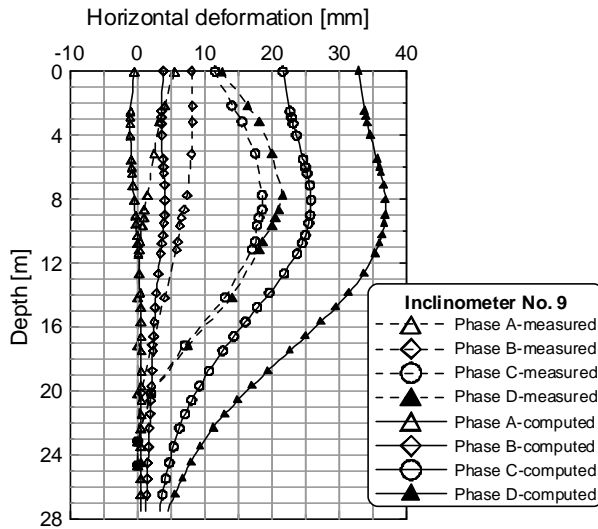

Figure 6: Comparison of the measured and computed deformations

In comparising of the measured and computed values, however, the assumption should be taken into consideration, that the toe of the wall is fixed in the evaluation of the inclinometer data. In reality, however, there always exists a horizontal movement of the toe of the wall in-situ, which is also Shown by the FEM-results. Therefore, the additional toe displacement of about 5 mm in (Phase C) should be taking into account in the evaluation of the inclinometer result. In respect to the excavation phase C, a deformation increment of about 20 mm was calculated up to the end of the excavation.

Both analytically and numerically computed anchor forces and the corresponding maximum bending moment at the end of the respective excavation phase are given in Table 2. At the end of the final excavation, a maximum bending moment of 900 kNm/m and a maximum anchor force of about 500 kN were determined.

As already mentioned in section 4, a safety analysis of the over all system was conducted using the Phi-c-reduction concept and the result shows a global safety factor of $\eta = 2.5$.

Table 2: Comparison of the measured and computed anchor forces and bending moments

Construction stages	Analytical		Numerical		Measured
	Anchor force [kN]	Bending moment [kNm/m]	Anchor force [kN]	Bending moment [kNm/m]	Anchor force [kN]
Phase C	590	890	606	808	-
Phase D	590	840	545	803	523,4
Phase E	595	790	599	919	555,0

6 ANALYSIS OF THE RESULTS AND CONCLUSION

Generally, the numerical results show a good agreement with the measured values, specially when the additional in-situ wall toe displacement is taken into consideration in the analysis of the inclinometer measurements.

The reason for the relatively small measured deformation in comparison to the computed values may lie on the favourable geometrical situation in-situ, the possibility of an uncompleted consolidation process (excess pore pressure might still exist in some layers at the end of the excavation) and the necessary approximation of some input parameters.

Despite the required simplification and assumptions made, it can generally be asserted on the basis of the good agreement and convergence of the results, that the FE-model as well as the obtained computation results are reasonable and realistic. They can be used as basis for the decision of further construction and design measures as it was the case in this project.

Based on the numerical results, it can be confirmed that there is an additional significant influence due to the displacement and deformation of the soil body between the diaphragm wall and the centre of the fixed length of the ground anchor, which acts as cofferdam. These horizontal displacements and deformations can not be determined using the standard analytical procedures, however, they can be estimated either by means of the FE-computations or an appropriate analytical approximations method (see for example, Gebreselassie & Kempfert 2004, Kempfert et al. 2000, Kempfert & Raithel 1998, Ulrichs 1981, Stroh 1974, Nendza & Klein 1974).

Since a good agreement was achieved between the measured and computed deformation of the wall, new observation and limit values were derived and it was able to safeguard the safety of the excavation and the cofferdam during the entire construction and utilisation phases. Fig. 7 shows the last excavation step.

Figure 7: Excavation pit

REFERENCES

Gebreselassie, B. and Kempfert, H.-G. 2004. Case history of a deep multi-tied-back excavation. *Proceedings of the International Conference on Structural and Foundation Failures, Singapore, pp. 466-474.*

Gebreselassie, B. 2003. Experimental, analytical and numerical investigations of excavations in normally consolidated Soft Soils. *Schriftenreihe Geotechnik. Universität Kassel, Heft 14.*

Kempfert, H.-G., Gebreselassie, B and Raithel, M. 2000. Damage on deep, multi-tied-back excavation due to the deformation of the anchor soil block system. *Proceedings of the International Conference on Geotechnical & Geological Engineering, GeoEng 2000. Melbourne*

Kempfert H.-G., Raithel M. 1998. Schäden an tiefen, rückverankerten Baugruben durch Verformungen des Systems Bodenblock-Verankerung. *Proceedings of the Christian Veder Kolloquium in Graz, Austria.*

Vermeer, P.A., Brinkgreve R.B.J. 1998. PLAXIS, Finite Element Code for Soil and Rock Analyses; *Balkema, Rotterdam-Brookfield.*

Ulrichs, K.R. 1981. Untersuchungen über das Trag- und Verformungsverhalten verankerter Schlitzwände in rolligen Böden. *Die Bautechnik, pp. 142.*

Stroh, D. 1974. Berechnung verankerter Baugruben nach der Finite Elemente Methode. *Mitteilungen der Versuchsanstalt für Bodenmechanik und Grundbau, TH Darmstadt, Heft 13.*

Nendza, H. and Klein ,K. 1974. Bodenverformung beim Aushub tiefer Baugruben. *Straße Brücke Tunnel 9; pp. 231.*